



# High-performance and low-cost ion sensitive sensor array based on self-assembled graphene

Bo Zhang, Tianhong Cui\*

Department of Mechanical Engineering, University of Minnesota, 111 Church Street S.E., Minneapolis, MN 55455, USA

## ARTICLE INFO

### Article history:

Available online 12 September 2011

### Keywords:

Ion sensitive sensor array

Graphene

Self-assembly

Sweat *in vitro* testing

## ABSTRACT

The ion sensitive sensor array (ISSA) based on layer-by-layer (LbL) self-assembled graphene presented in this paper is capable of detecting different ions selectively with advantages of high sensing performance and low cost due to graphene inherent properties and self-assembly technique. According to the conductance change of graphene, the detection limit of ISSA is down to 1  $\mu$ M, much better than one dimensional carbon nanotube (CNT) sensors. The response time of ISSA is 15 s. The human sweat *in vitro* testing also confirms the high performance of ISSA.

© 2011 Elsevier B.V. All rights reserved.

## 1. Introduction

Homeostatic regulation of ions, such as sodium, potassium, calcium, and hydrogen, is very critical for most cellular functions, especially for the stability of a human body system. Imbalance of these ions in a human body may cause diseases including heart failure ( $\text{Na}^+$ ,  $\text{K}^+$ ,  $\text{Ca}^{2+}$ ), hypertension ( $\text{Na}^+$ ,  $\text{K}^+$ ), kidney disease ( $\text{Na}^+$ ,  $\text{Ca}^{2+}$ ), etc. Therefore, testing and monitoring concentration of these ions in a human body play a very significant role in an early diagnose and control of relevant diseases. However, the prevailing methods for ion sensitive sensing such as ion sensitive electrodes [1] and radio isotopic tracer [2] suffer from a low selectivity of sensing multiple ions or very long response time, and most of them are expensive and complex.

To overcome the hurdles of these previous ion sensitive sensing methods, the layer-by-layer (LbL) self-assembled graphene is introduced to the ion sensitive sensing applications in this work. Due to its unique structural, electrical, chemical, and mechanical properties [3], graphene has attracted more and more attention these days. With rational chemical and/or physical modification, graphene is capable of detecting many types of molecules and ions [4,5]. The ion sensitive sensor array (ISSA) based on LbL self-assembled graphene provides a promising way to selectively sense different ions simultaneously with a very short response time and a very low detection limit due to its ultra high electron mobility and chemical sensitivity [6]. The ISSA based on LbL self-assembled graphene is designed to selectively detect multiple ions in a testing solution. Moreover, with the LbL self-assembly technique and the polyethylene

terephthalate (PET) substrate, ISSA has a high performance with much more mechanical flexibility and very low cost, compared with silicon based ion sensitive sensors. In addition, carbon nanotube (CNT) based ISSA under the same design, fabrication, and measurement conditions were also characterized, demonstrating that CNT was inferior to graphene with respect to detection limit. To further confirm the performance of graphene ISSA, human sweat *in vitro* testing was also conducted.

## 2. Design and fabrication

As shown in Fig. 1, different polyions and graphene nanoplatelets are deposited into the 20  $\mu$ m gaps between the sensor electrode arrays by self-assembly technique. A layer of PET constraining the sensing region of ISSA acts as a confinement layer. Different ionophores coated on the sensing region only allow matched ions to pass through the ionophore layer. Due to the absorption of ions, the conductance of graphene will change with the ion concentrations [7].

Microfabrication was utilized to pattern the electrodes of ISSA, and graphene layers were deposited by self-assembly technique. As is shown in Fig. 2, chromium/gold layers 50/200 nm thick were firstly deposited on a clean PET wafer with an AJA sputter system. Subsequently, sensor electrodes were patterned by photolithography. Another lithographic step was used to fabricate a window area on which the graphene film was self-assembled, while protecting the testing pads from the adsorption of graphene solutions. The polyelectrolytes used in this study were poly(diallyldiamine chloride) (PDDA) and poly(styrene sulfonate) (PSS), purchased from Sigma–Aldrich Inc. The concentrations of aqueous PDDA and PSS were 1.5 and 0.3 wt% respectively, with an addition of 0.5 M sodium chloride to enhance the surface properties. Research

\* Corresponding author. Tel.: +1 612 626 1636; fax: +1 612 625 6069.  
E-mail address: [tcui@me.umn.edu](mailto:tcui@me.umn.edu) (T. Cui).

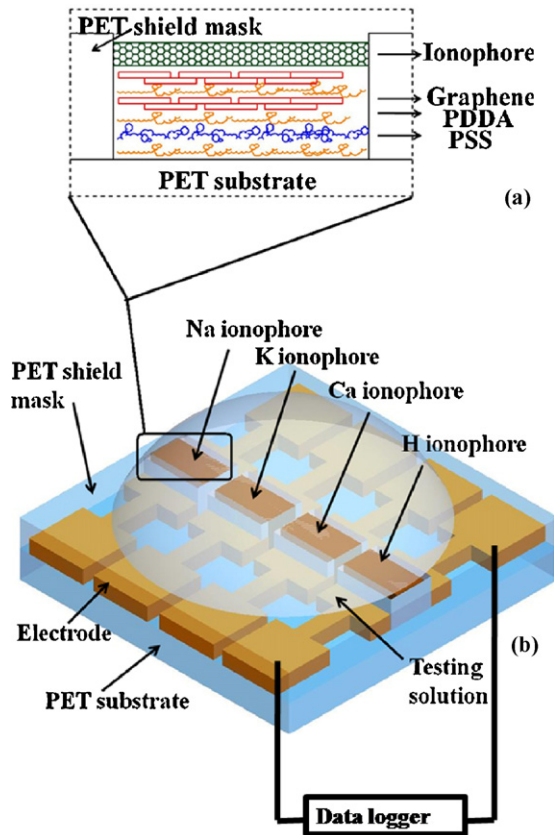


**Fig. 1.** (a) Structure of ISSA sensing region; (b) schematic of an ISSA: when a testing solution contains one type of ion, only the sensing channel with a matched ionophore triggers a signal. The conductance of the graphene layer is recorded by a data logger directly.

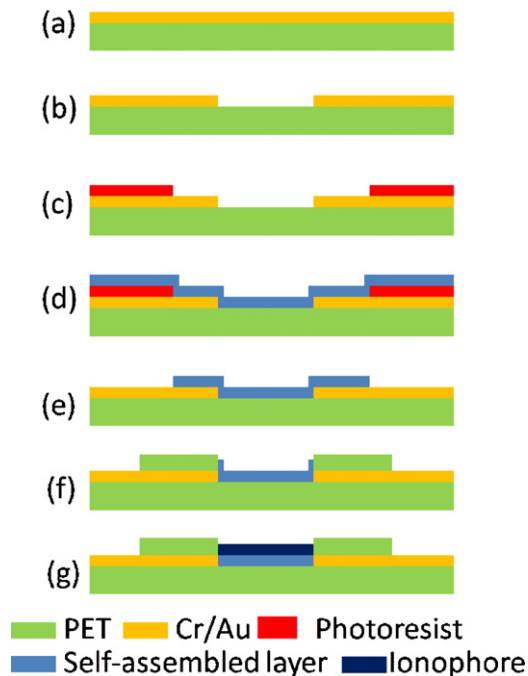


**Fig. 2.** (a) Cr/Au layers were sputtered on a cleaned PET substrate; (b) electrodes were patterned by photolithography; (c) a window area was fabricated by photolithography, protecting the test pads from the adsorption of graphene or CNT solutions; (d) self-assembly of graphene or CNT; (e) lift off; (f) another layer of PET was bonded with the substrate to confine the sensing regions; (g) ionophores were applied.

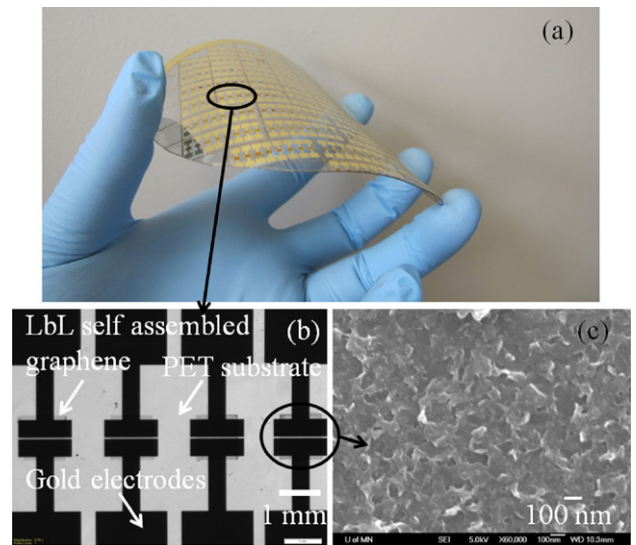


**Fig. 3.** (a) Image of ISSA on a flexible PET substrate; (b) optical image of ISSA; (c) SEM image of LbL self-assembled graphene layer, showing that the average size of graphene sheets is about 100 nm × 100 nm.

grade graphene (PureSheets™, 0.25 mg/ml) and carbon nanotube suspension solutions (PureTube™, 0.25 mg/ml) were purchased from Nanointegris Inc. Next, the substrate was immersed into the charged suspensions with a sequence of the immersion [PDPA (10 min) + PSS (10 min)]<sub>2</sub> + [PDPA (10 min) + graphene/CNT suspension (20 min)]<sub>5</sub>. Afterwards the substrate was immersed into acetone for 5 min to lift off the photoresist mask, and the flexible graphene sensors were inspected by scanning electron microscopy (SEM) (Fig. 3). Another layer of PET diced by a laser cutter was bonded with the substrate to confine the sensing regions. Different types of ionophores (potassium ionophore, sodium ionophore, calcium ionophore, and hydrogen ionophore,

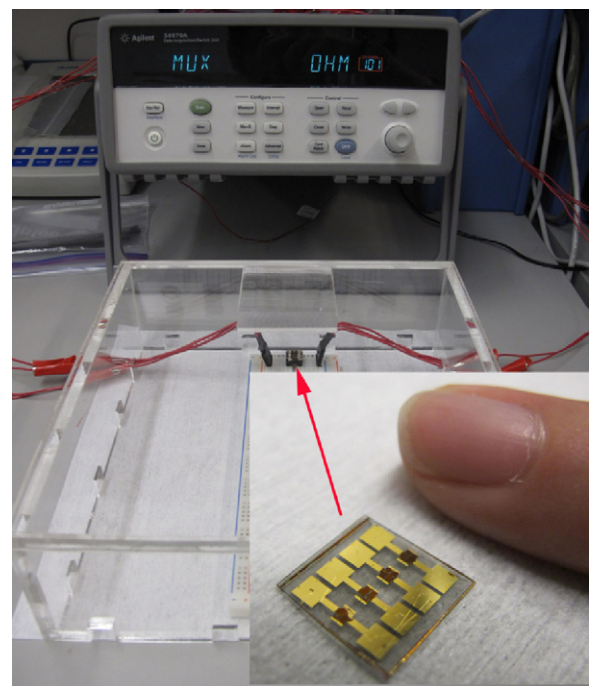


**Fig. 4.** Image of measurement setting up. The ISSA was connected to Agilent data logger, and the signals of the four testing channels were recorded simultaneously. Inset: image of packaged ISSA.

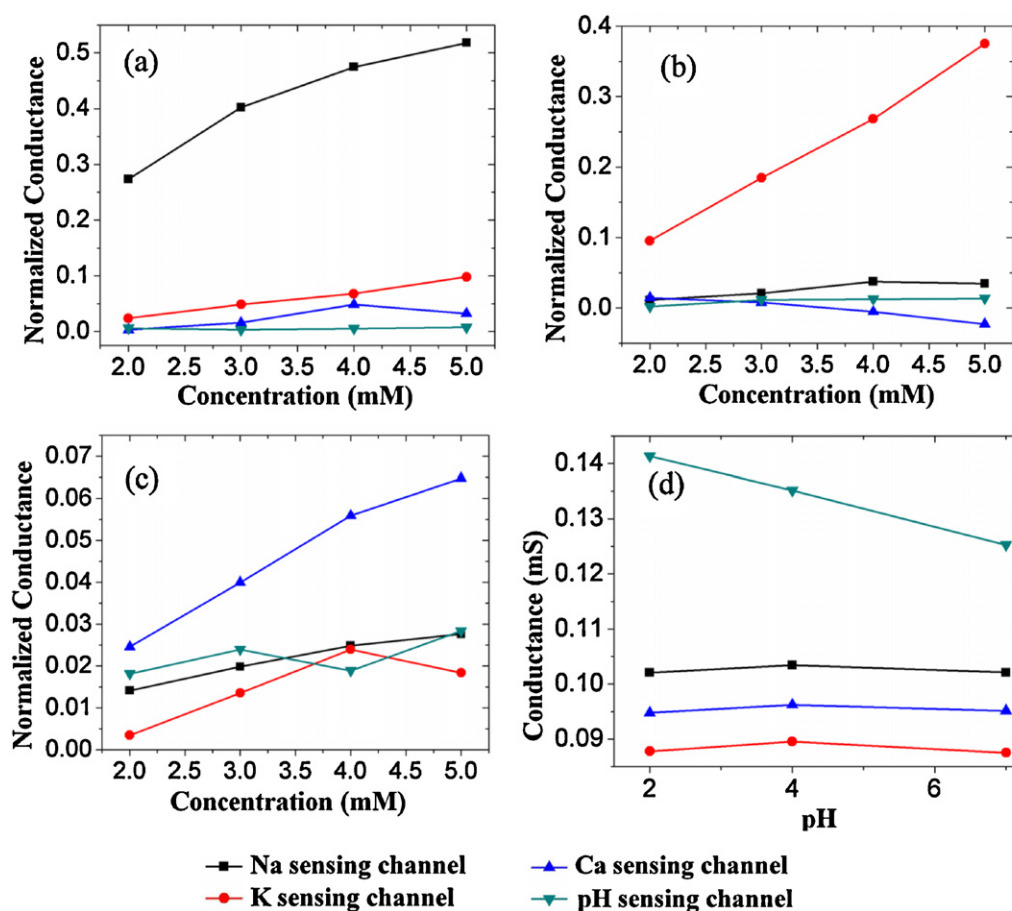


Fig. 5. Output results when testing solution contains (a) NaCl; (b) KCl; (c) CaCl<sub>2</sub>; (d) HCl.

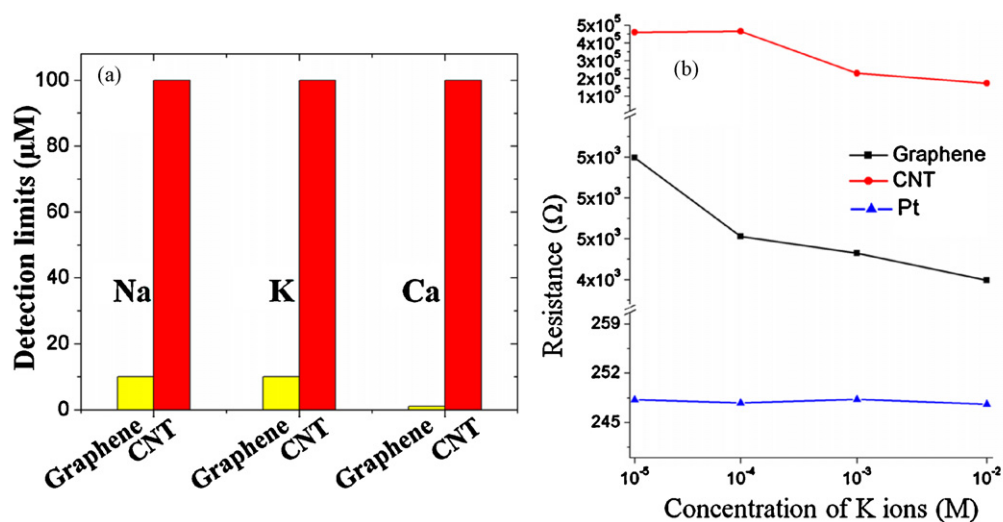


Fig. 6. (a) Detection limits compare between graphene and carbon nanotube for different ion testing. The detection limit of graphene ISSA is much better than CNT ISSA. (b) The resistance shifts of graphene, CNT and Pt based ISSA on K<sup>+</sup> testing, similar to the results of other ions.

Sigma–Aldrich Inc) were coated on the sensing regions respectively.

### 3. Results and discussion

For the characterization of ISSA, different concentrations of various ions were introduced to the sensing regions, and the

conductance shift of LbL self assembled graphene was monitored by an Agilent data logger (Fig. 4).

In order to investigate the selectivity of the ISSA, the testing solution containing one type of ions was applied to the ISSA, and the conductance of channels coated with different ionophores were recorded. As is shown in Fig. 5, the LbL self-assembled graphene conductance increases when absorbing these penetrating ions.

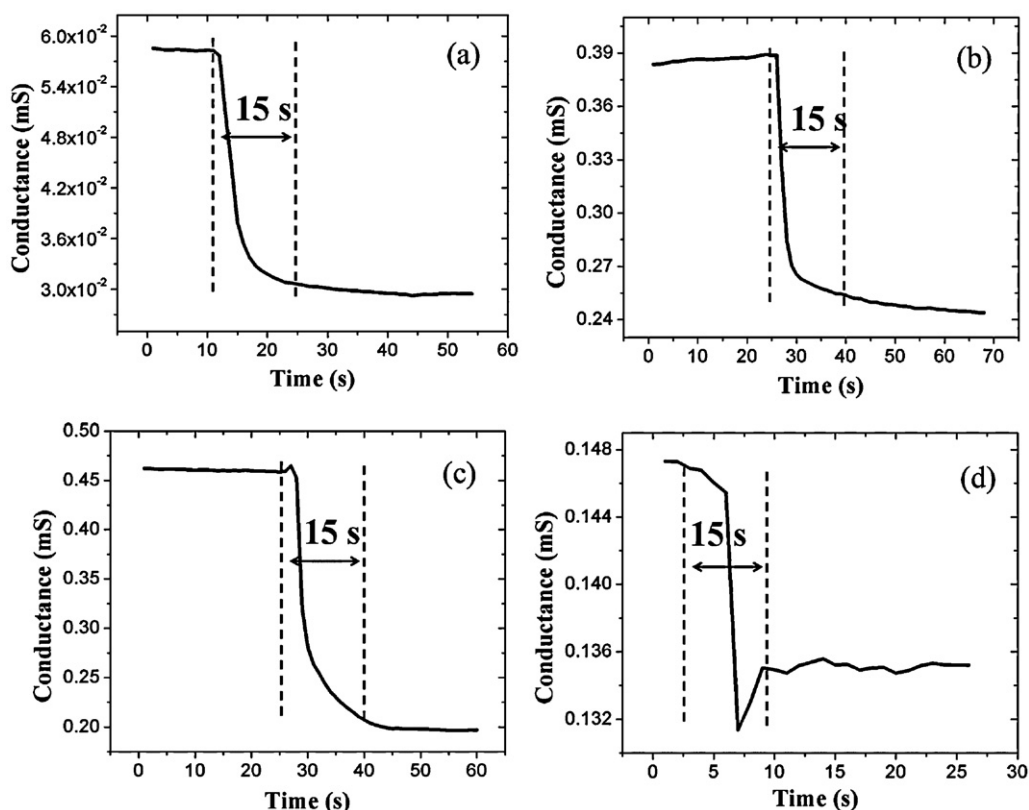


Fig. 7. Response time for 1 mM different ions testing: (a) Na; (b) K; (c) Ca; (d) H.

Different sensing ionophore channels had the corresponding signals representing the ion concentrations in the testing solution. In order to get an obvious readout, a normalized conductance was deduced. Conductance for a solution concentration of 1 mM was used as an initial conductance  $G_0$ , and other conductance tested under different concentrations subtracted  $G_0$  to get  $\Delta G$ . Normalized conductance was represented as  $\Delta G/G_0$ .

It is evident that a change in density and/or mobility of charge carriers must be responsive when ions are absorbed by graphene [7], reflected on the shift of conductance of graphene. The equation  $\sigma = nqv$  can demonstrate the relationship, where  $\sigma$  is conductance,  $n$  is carrier density,  $q$  is charge per carrier, and  $v$  is the carrier mobility. The charged ions absorbed by LbL self-assembled graphene increase the carrier density of graphene, in the chemical equivalent of the electric-field effect [8]. Moreover, they are serving to partially neutralize the Coulomb scatters induced by the substrate, allowing a rapid increase in electrical mobility. According to the conductance calculation equation above, both of the mechanisms increase the conductance with the absorption of hydrogen from the biocatalyzed reaction. The conductance of the graphene shifts with the concentration changes of different ion solutions. As is shown in Fig. 6(a), the detection limit of LbL self-assembled graphene based ISSA was characterized, and compared with the results of typical CNT composite ISSA under the same conditions of design, manufacture, and measurement. When changing different concentrations of ions, the graphene conductance was recorded by an Agilent data logger. The detection limits of different ions were determined by the lowest concentration detected by the ISSA. It is observed that the graphene ISSA has a much lower detection limit than the CNT composites for ion detection limits. In order to confirm the function of graphene ISSA, similar sensor array with platinum (Pt) as sensing material was tested. As is shown in Fig. 6(b), the graphene sensors showed the best performance, Pt sensors did not work well.

The low detection limit of graphene sensors was attributed to its inherent properties. Due to the crystal lattice and two-dimensional nature, graphene tends to screen charge fluctuations more than one-dimensional materials such as carbon nanotubes. The low  $1/f$  noise of graphene results in the better performance in detection limit. Moreover, two-dimensional structure gives rise to more exposure to ions, providing the greatest sensing area per unit volume for graphene [6]. These two factors operated together to promote the lower detection limit of graphene.

In addition, the response time of a graphene ISSA was tested by induced multiple ions. As shown in Fig. 7, 1 mM different ions were applied to the ISSA, and the conductance versus time data was recorded. The response time was determined by the duration from the steady states before and after the solution was applied. The response time was about 15 s, much faster than any other ion sensitive sensor. The reason is that the charge carriers of graphene have zero rest mass and travel rapidly, at approximately three one thousandths of the speed of light, through its honeycomb lattice [3]. The carrier transport time would be extremely fast due to the graphene properties in nature. Therefore the response time was primarily determined by the time consumed for penetration and absorption of ions.

In the meanwhile, human sweat *in vitro* testing was executed with the graphene ISSA, demonstrating that the ISSA was potentially an efficient and low-cost method for sweat testing in human health monitoring. Nowadays, several serious diseases such as cystic fibrosis (CF) were diagnosed by sweat testing method [9]. However, the traditional sweat testing suffered from the time consuming and large sweat sample amount (at least 100  $\mu$ l), which limited applications of sweat testing greatly. Herein, the graphene ISSA tested the concentrations of sodium ions in diluted human sweat from 0.1% to 100% (volume ratio), comparing with the same diluted 39 mM NaCl solution, the normal concentration of sodium ions in human body. The sweat samples were gathered from 3



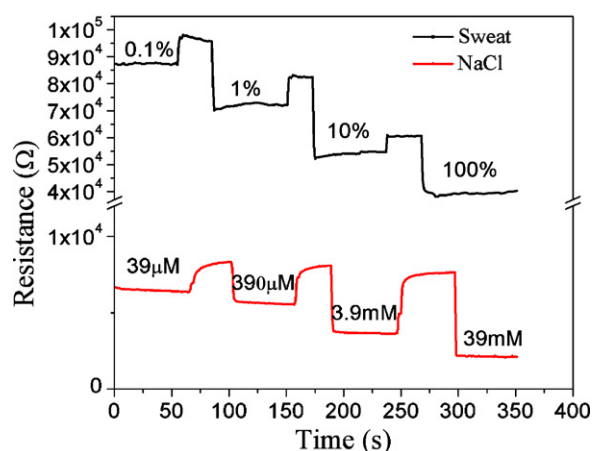


**Fig. 8.** Resistance of the graphene ISSA versus time for ISSA with different dilution rates of human sweat and NaCl. After alternate delivery of the different concentrations of NaCl solution and different diluting rates of sweat, the resistance of graphene ISSA decreases accordingly.

healthy males after exercising, and stored in a refrigerator. As shown in Fig. 8, the resistance of graphene diversifies as the variety of diluting rate in human sweat and NaCl solutions in time domain. After the results were normalized, the resistance shifted from 1% diluting rate to the original solution for human sweat and NaCl solution were compared. The difference between human sweat and NaCl solution at 1% diluting rate is only 1.06%. It demonstrates that the ISSA can successfully detect the sodium ion concentration in diluted sweat, which means that it requires smaller amount of sweat sample (about 10  $\mu$ l). Considering the fast reaction time, the graphene ISSA may overcome the hurdles of sweat testing by detecting diluted sweat in very short time.

#### 4. Conclusions

A flexible, low-cost, and high-performance ISSA was built and investigated in this paper. It was characterized by applying testing solutions containing certain ions to the sensor array. It was learned that the LbL self-assembled graphene conductance increases when absorbing the penetrating ions, and different sensing ionophore

channels output the corresponding signals representing the ion concentrations in the testing solution. It was also learned that the response time of an ISSA is about 15 s, much faster than other ion sensors. In addition, the detection limit of the ISSA based on graphene is 1–10  $\mu$ M, which is much better than carbon nanotube composite as a sensing material under the same conditions. Moreover, the human sweat *in vitro* testing shows that the ISSA provides a promising potential technique for clinical sweat diagnosis. The results presented herein suggest a new route to an inexpensive and high-performance ISSA for biochemical sensing applications.

#### Acknowledgements

The authors acknowledge the assistance of fabrication and characterization from Nanofabrication Center and the Characterization Facility at the University of Minnesota. The authors acknowledge Dr Min Zhang's assistance in SEM imaging. The authors also thank Professor William R. Kennedy for his valuable discussion on sweat sampling and testing.

#### References

- [1] J. Philippe, N. Epoy, J. Guicquero, Nano-pH sensor for the study of reactive materials, *Anal. Chem.* 79 (2007) 7560–7564.
- [2] J. Becker, D. Pozebon, J. Becker, LA-ICP-MS studies of zinc exchange by copper in bovine serum albumin using an isotopic enriched copper tracer, *J. Anal. Spectrom.* 23 (2008) 1076–1082.
- [3] K.S. Novoselov, A.K. Geim, S.V. Morozov, D. Jiang, Y. Zhang, S.V. Dubonos, I.V. Grigorieva, A.A. Firsov, Electric field effect in atomically thin carbon films, *Science* 306 (2004) 666–669.
- [4] Y. Ohno, K. Maehashi, K. Matsumoto, Electrolyte-gated graphene field-effect transistors for detecting pH and protein adsorption, *Nano Lett.* 9 (2009) 3318–3322.
- [5] B. Zhang, T. Cui, High-performance and low-cost ion sensitive sensor array based on self-assembled graphene, in: *IEEE MEMS 2011 Conference, Cancun, Mexico* January 23–27, 2011, pp. 497–500.
- [6] J.D. Fowler, M.J. Allen, V.C. Tung, B.H. Weiller, Practical chemical sensors from chemically derived graphene, *ACS Nano* 3 (2009) 301–306.
- [7] K. Ratnac, W. Yang, S. Ringer, F. Braet, Toward ubiquitous environmental gas sensors capitalizing on the promise of graphene, *Environ. Sci. Technol.* 44 (2010) 1167–1176.
- [8] F. Schedin, A.K. Geim, S.V. Morozov, E.W. Hill, P. Blake, M.I. Katsnelson, K.S. Novoselov, Detection of individual gas molecules adsorbed on graphene, *Nat. Mater.* 6 (2007) 652–655.
- [9] B.J. Rosenstein, G.R. Cutting, The diagnosis of cystic fibrosis: a consensus statement, *J. Pediatr.* (1998) 589–595.